Carrier relaxation and recombination in InGaN/GaN quantum heterostructures probed with time-resolved cathodoluminescence

Xingang Zhang*, D. H. Rich*, J. T. Kobayashi*, N. P. Kobayashi*, P. D. Dapkus**
*Department of Materials Science and Engineering, University of Southern California, Los Angeles, CA 90089-0241
**Also with Department of Electrical Engineering/Electrophysics, University of Southern California, Los Angeles, CA 90089-0271

ABSTRACT

Spatially, spectrally, and temporally resolved cathodoluminescence (CL) techniques have been employed to examine the optical properties and kinetics of carrier relaxation in InGaN/GaN heterostructure and single quantum well (QW) samples. CL images of the QW sample revealed a spotty cellular pattern indicative of local In compositional fluctuations on a scale of < 100 nm. The compositional variations induce local potential fluctuations, resulting in a strong lateral excitonic localization at InN-rich regions in the InGaN QW layer. Time-resolved CL measurements revealed a lateral spatial variation in the luminescence decay time which correlates with the spatial variation in the luminescence efficiency. A reduced lifetime is observed at boundary regions between centers of excitonic localization. A detailed time-resolved CL study shows that carriers generated in the boundary regions will diffuse toward and recombine at the InN-rich centers. An electron beam induced modification of the emission spectra was observed for InGaN/GaN heterostructure samples. Exposure to the e-beam resulted in a shift in the near-band gap emission to higher energies with a simultaneous increase in the emission intensity. These result are interpreted as a modification of the surface passivation through e-beam exposure and carbidization of the surface.

INTRODUCTION

The study of InGaN/GaN heterostructures and QWs has received a great deal of interest recently because of rapid progress and realization of high quality blue and green InGaN single QW light emitting diodes[1] and room-temperature pulse oscillation of InGaN single[2] and multiple[3] QW laser diodes. Time-resolved photoluminescence has been used to study the radiative recombination in InGaN single[4,5] and multiple[6] QW structures. Several authors observed that the emission results mainly from recombination of excitons localized at certain potential minima originating from a large $In_xGa_{1-x}N$ compositional fluctuation.[6-8] Direct evidence for exciton localization was shown in InGaN single QWs by Chichibu *et al.*[9] However, the details of the carrier diffusion and capture process, and the relaxation of localized excitons are far from being well understood, particularly in the boundary regions between centers of exciton localization.

In this study, we have employed spatially, spectrally, and temporally resolved cathodoluminescence (CL) to investigate the carrier relaxation and recombination in InGaN/GaN heterostructues and single QW samples. The impact of the large $In_xGa_{1-x}N$ compositional fluctuations on the spatial variation in the luminescence intensity and lifetime is explored. Quantitative lifetime information is obtained in connection with these spatial variations. The sensitivity of the optical behavior to electron beam bombardment is further explored in an InGaN/GaN heterostructure sample. The results reveal that details of the surface passivating layer can have large effects on the subsequent luminescence properties.

EXPERIMENTAL

A 7-nm-thick InGaN single QW sample was studied here. The sample was grown by atmospheric pressure metalorganic chemical vapor deposition (MOCVD) using a closed space showerhead reactor via multi-step growth approach[10] on a sapphire (0001) substrate, followed by a 70-nm-thick GaN capping layer. The InGaN/GaN heterostructure was grown under conditions similar to the QW, but without a GaN cap layer. All samples were undoped and have a 16% average In composition.

The CL experiments were performed with a modified JEOL-840A scanning electron microscope (SEM) using a 15 keV electron beam with various probe currents.[11,12] The temperature of the sample was maintained at 87 K. Our CL system with time-resolved capability has been described previously[12] and time-resolved CL experiments were performed with the method of delayed coincidence in an inverted single photon counting mode, with a time resolution of ~100 ps. Electron beam pulses of 50 ns width with a 1 MHz repetition rate were used to excite the sample. The luminescence signal was dispersed by a 0.25-meter monochromater and detected by a cooled GaAs:Cs PMT. Time-delayed CL spectra were acquired with a spectral resolution of ~1 nm.

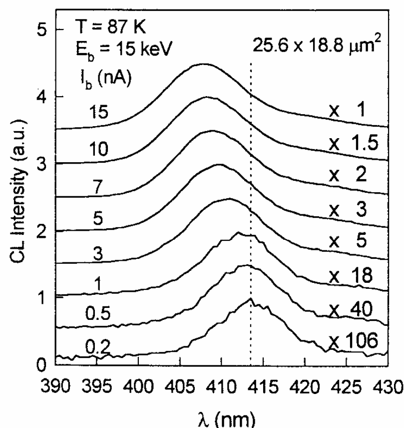

Figure 1. Stack plots of normalized CL spectra for InGaN/GaN QW sample using various probe currents.

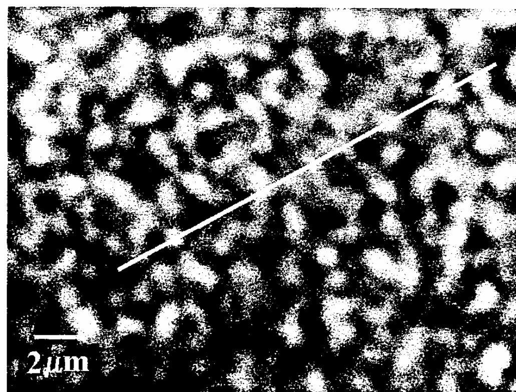

Figure 2. Monochromatic CL image of the InGaN/GaN QW (λ= 410 nm) sample.

RESULTS AND DISCUSSION

Spatially averaged CL spectra of the QW sample, acquired under various excitation currents (I_b), are shown in Fig. 1. The beam currents vary from 0.2 to 15 nA and the beam was raster scanned over an area of 25.6 X 18.8 μm^2. All spectra are normalized to have the same intensity; the scaling factors are indicated to the right of each spectrum. The peak position of the QW emission shifts toward shorter wavelengths as the beam current increases, resulting in a ~36 meV blue-shift as the beam current is increased from 0.2 to 15 nA. This effect can be attributed to the

rapid band filling of localized $In_xGa_{1-x}N$ radiative centers composed of large In concentrations. The full widthss at half-maxmum (FWHM) of these spectra also increase from 76.6 to 87.5 meV in the 0.2 to 15 nA range.

A scanning monochromatic CL image (λ = 410 nm) of this same region is shown in Fig. 2. The spotty nature of the CL image, showing distinct bright and dark emission regions, is consistent with a strong localization of excitons prior to radiative recombination.[10] The minimum lateral size of these islands is estimated at ~0.1 μm. The actual size of the In-rich regions cannot be determined from the present data, owing to the 50-100 nm carrier diffusion length which limits the spatial resolution in CL imaging.[7,9]

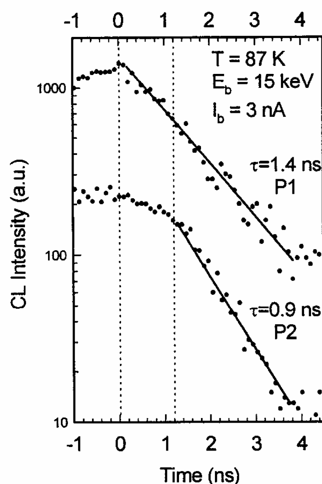

Figure 3. CL transients of the 410 nm luminescence taken near an exciton localization center (P1) and a boundary (P2).

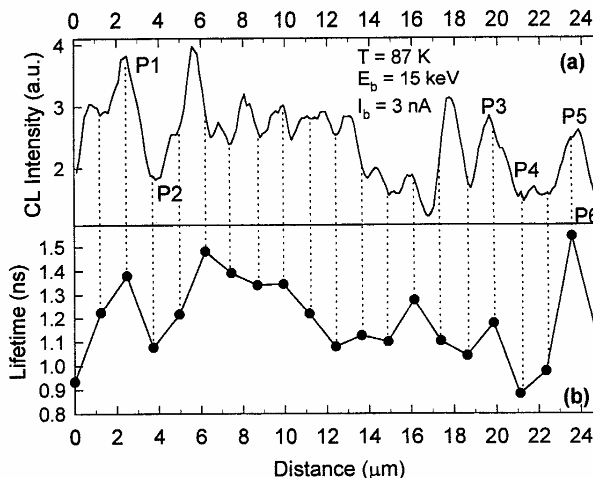

Figure 4. CL intensity (a) and lifetimes (b) vs distance for an e-beam line scan.

In order to further understand the spatial variation in the carrier relaxation and recombination, time-resolved CL was performed by positioning the e-beam in varying proximity to the bright luminescence centers and dark boundary regions observed in Fig. 2. Transients of the CL intensity decay vs time were acquired at various positions relative to exciton localization centers. Figure 3 shows typical transients, denoted as P1 and P2, corresponding to the e-beam positioned to a bright center and dark boundary region, respectively. The CL decay lifetimes are determined from the slopes, in the usual manner, by a linear fit to the log(intensity) vs time data, as shown by the lines in the semi-logarithmic plots of Fig. 3. The fits indicate that the region corresponding to P1 exhibits a longer lifetime (1.4 ns) than the region corresponding to P2 (0.9 ns). A spatial dependence of the lifetime was examined by acquiring a set of transients along an arbitrary line in an e-beam line scan. Figure 4(a) shows a line scan analysis of the CL intensity, at λ = 410 nm, for an arbitrary line scan of ~24.5 μm in length, taken along the regions indicated by the white line in Fig. 2. The peaks and valleys in Fig. 4(a) correspond to the luminescence centers (bright regions) and boundaries (dark regions), respectively, in the CL image of Fig. 2. The dots in Fig. 4(b) show the corresponding decay times of the 410 nm emission at various e-beam positions along the same line. The positions of the transients denoted as P1 and P2 in Fig. 3

are also indicated in Fig. 4.

A strong correlation is observed between the CL intensity and carrier lifetime in Fig. 4. The carrier lifetimes are generally longer and shorter for higher and lower CL intensities, respectively, along the line scan. The reduced lifetime in the darker boundary regions can be attributed to defects and/or impurities which act as nonradiative centers which reduce the total lifetime of excess carriers.

A closer examination of the CL transients P1 (bright region) and P2 (dark region) in Fig. 3 shows marked differences during the initial stages of the intensity decay. The decay of P1 follows an exponential behavior beginning with the trailing edge of the e-beam pulse (time≈0). For P2, however, the CL intensity decays slowly during the first ~1.2 ns after the trailing edge of the e-beam pulse and then proceeds to decay exponentially. This unusual decay behavior was observed consistently for other dark valley regions which were found in close proximity (1-2 μm) of sharp peaks, such as for the P3/P4 and P5/P6 pairs denoted in Fig. 4(a). This delayed time ranged from 0.2-1.2 ns.

The delay can be explained by considering a simple model that involves carrier generation in dark boundary regions and transport to the lower bandgap InN-rich centers that yield the high exciton localization. At the trailing edge of the e-beam excitation, excess carriers can diffuse and drift from the higher to lower bandgap regions. The In composition undulation will likewise introduce a bandgap variation which will create minima in the potential at InN-rich centers. Thus, we expect the field-induced drift of carriers to play an important role in funneling and collection of carriers at the InN centers. At the trailing edge of the e-beam pulse, generated carriers in the higher band gap dark regions must traverse the 1-2 μm distance prior to collection and recombination in the InN-rich centers. This process gives rise to an apparent 0.2-1.2 ns delay in the CL transient as carriers are continuously fed to the luminescence centers. The relative proximity of the e-beam position to the centers will influence the measured delay. After transporting to the InN-rich centers, the carriers can recombine radiatively. Owing to possible nonradiative centers in the boundary regions, carrier loss during transport is expected to occur and contributes to the reduced lifetime measured in dark regions. The rapid band filling observed in Fig. 1 is also consistent with the notion of spatially segregated InN-rich centers with a high carrier collection efficiency. The collection of carriers at dispersed centers will naturally lead to an enhanced phase space filling due to the enhanced real space filling (i.e., funneling of carriers) in the centers. These results indicate a high capture and luminescence efficiency in InN-rich centers and further help to explain the high efficiency of optoelectronic devices based on InGaN alloys, despite high densities of structural defects.[13]

In order to further examine the carrier relaxation process, we have measured time-delayed CL spectra at 87 K for the various time windows indicated in Fig. 5. The beam was rastered over the same region as that of the CL

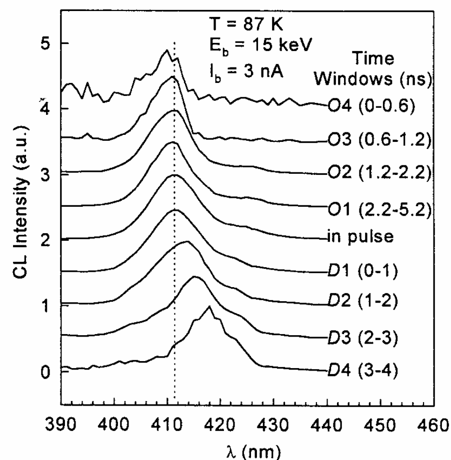

Figure 5. Time delayed CL spectra shown with various onset (Oi) and decay (Di) time windows. All spectra are renormalized to have about the same maximum peak height.

image in Fig. 2. The time windows *O*1 - *O*4 and *D*1 - *D*4 denote time windows relative to the beginning of onset and decay, respectively, of the luminescence, as referred to the beginning and end of the electron beam pulses. A rapid capture of carriers occurs, giving rise to a blue-shifted peak centered at 410 nm during the earliest onset window (*O*4) centered at 300 ps with regard to the leading edge of the e-beam pulse. At longer onset times, carriers begin to relax towards lower energy states as the carrier concentration approaches a steady state. A small red-shift of 2-4 nm is observed in the *in pulse* window relative to *O*4. The *in pulse* window refers to a 3-ns wide acquisition window centered in the middle of the 50-ns wide e-beam pulse. During the decay stage of the luminescence, a red-shift of main peak is detected in the *D1* - *D4* windows, reflecting the reduction in carrier concentration and reduced band filling at the InN-rich centers as the system approaches equilibrium. This red-shift is also consistent with the band filling behavior observed in the excitation dependent measurements of Fig. 1.

We also examined the optical properties of an InGaN/GaN heterostructure sample grown without a GaN cap layer, as shown in Fig. 6. The CL spectra *A*, *B*, *C*, *D* and *E* were taken consecutively over the same sample region with an area of 42.7 X 31.3 μm^2. Each CL spectrum was acquired consecutively in 150 s time intervals. There are two peaks in spectrum *A*, one is peaked at ~426 nm (*p1*) and the other is at ~450 nm (*p2*). There is a strong blue shift of ~37 nm with a concomitant ~6-fold increase in peak intensity for *p2* after a total exposure time of longer than 600s. After raising the sample to room temperature (RT) and re-cooling to 87 K, the CL spectrum was again acquired using the same conditions and is similar to *E*, indicating that this phenomenon could be irreversible. Deep levels are suggested to be responsible for the persistent photoconductivity effects in GaN.[14-16] Shmagin *et al.* observed that ultraviolet (UV) light of high power density can temporarily change the optical properties of InGaN epitaxial layer[17], leading to interesting read-write effects in UV optical microscopy. It is possible that the effect reported here is related to the filling and/or activation of trap levels. However, this effect is markedly reduced for InGaN QW samples which were subjected to similar e-beam exposure conditions. This leads us to conclude that the e-beam may influence the surface passivation conditions of the $In_xGa_{1-x}N$ layer by partially desorbing the oxide layer at the surface and/or leaving a carbon-based residue during exposure. Carbidization of a surface by persistent exposure to an electron beam is a well known problem that can afflict a variety of electron probes under varying vacuum conditions. In our case, the presence of carbon at the surface could significantly influence the band bending in the hetero-layer and attendant minority carrier recombination at the surface since the InGaN film has a thickness of only ~70 Å.

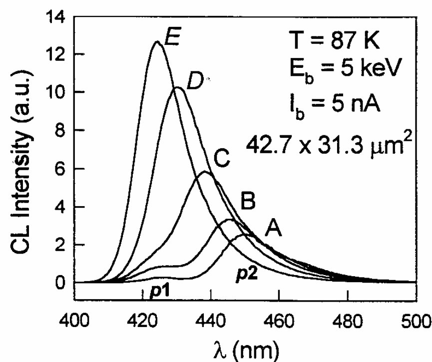

Figure 6. Effects of e-beam exposure on the optical properties of an InGaN/GaN heterostructure without a GaN cap.

CONCLUSIONS

In conclusion, we have examined the kinetics of carrier relaxation as well as optical properties of InGaN QW and InGaN/GaN heterostructure samples with spatially, spectrally, and temporally resolved CL. An exciton localization in InN-rich regions was observed in CL imaging

and spectroscopy, owing to the In composition undulation throughout the InGaN film. This composition modulation leads to a lateral bandgap variation throughout the QW. When carriers are excited in dark regions located between the InN-rich centers, the carrier lifetime is reduced and a 0.2-1.2 ns delay in the transient decay signal is observed owing to diffusion and drift of carriers. We found that a persistent e-beam exposure will modify the wavelength and intensity of luminescence for the InGaN/GaN heterostructure. No apparent e-beam-induced change in the optical properties was observed for the QW sample. The lateral InGaN phase segregation can lead to interesting nonlinear optical effects which could impact applications involving lasers, optical storage, and spatial light modulators.

ACKNOWLEDGEMENT

The authors acknowledge the support of the National Science Foundation, Army Research Office, Office of Naval Research, and DARPA through the National Center for Integrated Photonic Technology (NCIPT).

REFERENCES

1. S. Nakamura, M. Senoh, N. Iwasa, S. Nagahama, T. Yamada, and T. Mukai, Jpn. J. Appl. Phys. 1 **134**, L1332 (1994).
2. S. Nakamura, M. Senoh, S. Nagahama, N. Iwasa, T. Yamada, T. Matsushita, H. Kiyoku, and Y. Sugimoto, Appl. Phys. Lett. **68**, 3269 (1996).
3. I. Akasaki, S. Sota, H. Sakai, T. Tanaka, M. Koike, and H. Amano, Electron. Lett. **32**, 1105 (1996).
4. C.-K. Sun, S. Keller, G. Wang, M. S. Minsky, J. E. Bowers, and S. P. DenBarrs, Appl. Phys. Lett. **69**, 1936 (1996).
5. E. S. Jeon, V. Kozalov, Y.-K. Song, A. Vertikov, M. Kuball, A. V. Nurmikko, H. Liu, C. Chen, R. S. Kern, C. P. Kuo, and M. G. Craford, Appl. Phys. Lett. **69**, 4194 (1996).
6. Y. Narukawa, Y. Kawakami, S. Fujita, and S. Fujita, Phys. Rev. B **55**, R1938 (1997).
7. Y. Narukawa, Y. kawakami, M. Funato, S. Fujita, and S. Fujita, Appl. Phys. Lett. **70**, 981 (1997).
8. S. Chichibu, T. Azuhata, T. Sota and S. Nakamura, Appl. Phys. Lett. **69**, 4188 (1996).
9. S. Chichibu, K. Wada, and S. Nakamura, Appl. Phys. Lett. **71**, 2346 (1997).
10. J. T. Kobayashi, N. P. Kobaysahi, P. D. Dapkus, X. Zhang and D. H. Rich, Mater. Res. Soc. Symp. Proc. Vol. **468**. 187 (1997).
11. D. H. Rich *et al.*, Phys. Rev. B **43**, 6836 (1991).
12. H. T. Lin, D. H. Rich, A. Konkar, P. Chen, and A. Madhukar, J. Appl. Phys. **81**, 3186 (1997), and references therein.
13. S. D. Lester, F. A. Ponce, M. G. Craford and D. A. Steigerwald, Appl. Phys. Lett. **66**, 1249 (1995).
14. A. E. Wickenden, G. Beadie, D. D. Koleske, W. S. Rabinovich, and J. A. Freitas, Mater. Res. Soc. **449**, 531 (1997).
15. C. H. Qiu and J. I. Pankove, Appl. Phys. Lett. **70**, 1983 (1997)
16. V. A. Joshkin, J. C. Roberts, E. L. Piner, M. K. Behbehani, F. G. McIntosh, and S. M. Bedair, Appl. Phys. Lett. **71**, 234 (1997).
17. I. K. Shmagih, J. F. Muth, R. M. Kolbas, R. D. Dupuis, P. A. Grudowski, C. J. Eiting, J. Park, B. S. Shelton and D. J. H. Lambert, Appl. Phys. Lett. **71**, 1382 (1997).